THE ASTROPHYSICAL JOURNAL, 434:523–535, 1994 October 20

A *ROSAT* OBSERVATION OF THE NEARBY SPIRAL GALAXY NGC 6946

ERIC M. SCHLEGEL[1]
NASA/Goddard Space Flight Center, Code 668, Greenbelt, MD 20771;
eric@heasfs.gsfc.nasa.gov
Received 1993 October 6; accepted 1994 April 26

ABSTRACT

I present the *ROSAT* Position-Sensitive Proportional Counter image of the nearby, nearly face-on, spiral galaxy NGC 6946. The galaxy was observed with *Einstein* in 1980, uncovering a nuclear source, a source on or near the northern spiral arm, SN 1980K, and evidence for non–point-source (i.e., diffuse) emission. The *ROSAT* image resolves the nuclear region into approximately three sources, yields an accurate position for the north arm source, and reveals diffuse extended emission across the galaxy face, tracing at least the bright northern spiral arm of the galaxy. The diffuse emission is almost certainly the very hot component of the galaxy's interstellar medium and is probably similar to that found in the Milky Way and the Large Magellanic Cloud.

Subject headings: galaxies: individual (NGC 6946) — galaxies: nuclei — galaxies: spiral — X-rays: galaxies

1. INTRODUCTION

The X-ray study of nearby galaxies essentially started with the *Einstein* satellite (Fabbiano 1989, 1992). X-ray morphology studies using *Einstein* data were possible only for the nearest galaxies (e.g., M31, M33, M51, and the Large Magellanic Cloud [LMC]). The somewhat poor spatial resolution of the *Einstein* IPC made source identification difficult in dense source regions as, for example, in the plane of a galaxy. Regardless, our knowledge of the X-ray emission properties of galaxies advanced considerably. Normal galaxies were observed to emit X-rays with luminosities of $\sim 10^{38}$–10^{42} ergs s^{-1}. Observers are naturally interested in the origins of the observed X-ray emission. The *Einstein* results for late-type galaxies were generally consistent with the summed emission of unresolved point sources such as X-ray binaries. A question remains, however, whether a hot interstellar medium (ISM) in a spiral galaxy is detectable. The heating mechanism for a hot ISM is believed to be the energy input from supernovae (Fabbiano 1989).

Of the nearby galaxies available to the *Einstein* imaging proportional counter (IPC) for detailed studies, the X-ray emission of spiral galaxies such as M31 appears to be dominated by the summed emission from X-ray binaries while that of the LMC is dominated by supernova remnants (Fabbiano 1989, and references therein). The local galaxies thus suggest a correlation between the morphology of the galaxy and the galaxy's X-ray–emitting population. A cautionary note must be sounded, however. The inclination of a galaxy can be sufficiently high that a soft emission source may be completely extincted by the hydrogen column in the target galaxy, resulting in a potential bias toward harder sources. Face-on spirals are better targets to study the total X-ray–emitting population, including soft X-ray–emitting, point sources because the internal absorption or inclination effects are minimized. Face-on galaxies are of no value in studying extended hot halos because the halos are projected onto the disk and create confusion. As *ROSAT*'s energy band is relatively soft compared to previous missions, the study of face-on spirals becomes more important for a galaxy-wide population study.

[1] Also, Research Scientist, Universities Space Research Association.

The *ROSAT* Position-Sensitive Proportional Counter (PSPC) offers two very important advantages over previous X-ray observations of galaxies. First, the telescope-instrument combination has a very good angular resolution. While the on-axis FWHM at 1 keV is $\sim 26''$ (Hasinger et al. 1992), the position centroid is $\sim 5''$–$8''$ (Kürster & Hasinger 1993). Source identification for the brighter objects becomes possible as source confusion is reduced except in crowded regions. Second, the internal background of the PSPC is very low ($\sim 3 \times 10^{-5}$ counts s^{-1} $arcmin^{-2}$; Snowden et al. 1992) which permits a deeper probe of the X-ray luminosity function and the X-ray morphology of galaxies. In particular, the low background permits more galaxies to be surveyed more deeply than was possible with the *Einstein* IPC.

In this paper, I report here on the *ROSAT* PSPC observation of the nearby, nearly face-on Scd galaxy NGC 6946. This study is approximately equivalent to the *Einstein* IPC study of M33 (Trinchieri, Fabbiano, & Peres 1988). NGC 6946 lies at a relatively low galactic latitude ($b = 11^\circ.7$), so the galactic absorption column to the galaxy is moderately high ($\sim 5 \times 10^{21}$ cm^{-2}; Burstein & Heiles 1984). NGC 6946 is source 29 in the Atlas of Peculiar Galaxies (Arp 1966), largely because of its bright, northeastern spiral arm. It is a moderate starburst galaxy based upon studies by de Gioia-Eastwood, Grasdalen, & Strom (1984), Engargiola (1991), and Ishizuki et al. (1990). Ishizuki et al. find a strong concentration of H_2 in the nucleus formed by an efficient inflow; the existence of considerable activity in the nucleus is implied by this result. From H I studies, the inclination has been deduced to be $\sim 30^\circ$ (0° is face-on) (Rogstad, Shostak, & Rots 1973), although Tully (1988) lists the inclination as 42°. Kamphius & Sancisi (1993) have observed H I at high velocities and concluded that the emitting gas is located in the halo. The halo gas is swept out of the disk by the action of supernovae and stellar winds. Kamphuis & Sancisi speculate that all galaxies may behave in a similar manner. Klein et al. (1982), in a study at 2.8 cm, show that the thermal radio emission is clumpy; the clumps match the locations of H II regions. Tacconi & Young (1990) studied the azimuthal variations in the molecular and atomic components by comparing *B* and *I* images with H_2 and H I maps. NGC 6946 has been studied extensively in other bandpasses, with maps produced for the radio continuum (van der Kruit, Allen, & Rots 1977), CO emission (Young & Scoville 1982), Hα, the optical continuum (7020 Å) (Roy & Belley 1993), and [C II] 158 μm (Madden et al. 1993). Ehle & Beck (1993) have recently published a study of the intrinsic magnetic fields present in the galaxy.

The *Einstein* IPC was used to study NGC 6946 (Fabbiano & Trinchieri 1987, hereafter FT). Two sources were visible but barely resolved by the IPC's point-spread function. FT suggested the northern source was consistent with a thermal radio source observed by Klein et al. (1982). Too few counts existed for a spectral fit. The other source appeared coincident with the galaxy nucleus. A spectral fit was possible for the entire galaxy resulting in a thermal bremsstrahlung temperature of $kT \sim 0.8$ keV. This temperature is considerably softer than the typical temperature of the IPC-studied galaxies ($kT \sim 3$–5 keV) (FT; Kim, Fabbiano, & Trinchieri 1992). Radial profile plots of the southern portion of the disk showed emission inconsistent with a point source, thereby suggesting the possibility of diffuse thermal emission.

Distances used by the various authors have generally been around 10 Mpc, based upon the distance adopted in Rogstad et al. (1973). More recent work, based upon the brightest H II regions visible, has set the distance at 7 Mpc (Israel 1980). McCall (1982) used a value of 5.9 Mpc. In this paper, I assume a distance to NGC 6946 of 5.5 Mpc (Tully 1988). This distance translates to a scale of 26.6 pc arcsec^{-1}.

The plan of this paper is as follows. Section 2 will describe the observations and data analysis in detail. Section 3 will describe the individual sources found in the galaxy. Section 4 will describe the diffuse emission present, and § 5 discusses the results.

2. THE OBSERVATION

The *ROSAT* PSPC observed NGC 6946 on 1992 June 16–21, obtaining a total exposure time of 36,713 s scattered over 14 observation intervals. The mean count rate in each observation interval was calculated, as well as the mean of these means. Observation intervals in which an interval's mean count rate was more than 3 σ from the total mean count rate were screened out. A total of 70 s failed this criterion, leaving a total exposure time of 36,643 s. Figure 1 shows the raw data with the count-rate screening applied. The original pixels from the MPE SASS processing software are 0".5. The data in Figure 1 have been binned by a factor of 16, resulting in 8" pixels (all images in this paper will use 8" pixels). Note that no smoothing or background subtraction has been applied to the data in Figure 1. The quality of the *ROSAT* PSPC is immediately evident. Without additional work, we see that where the *Einstein* IPC showed two, barely resolved sources, the PSPC data show approximately five sources as well as possible diffuse emission with an apparent spiral morphology.

The background light curve was examined as recommended

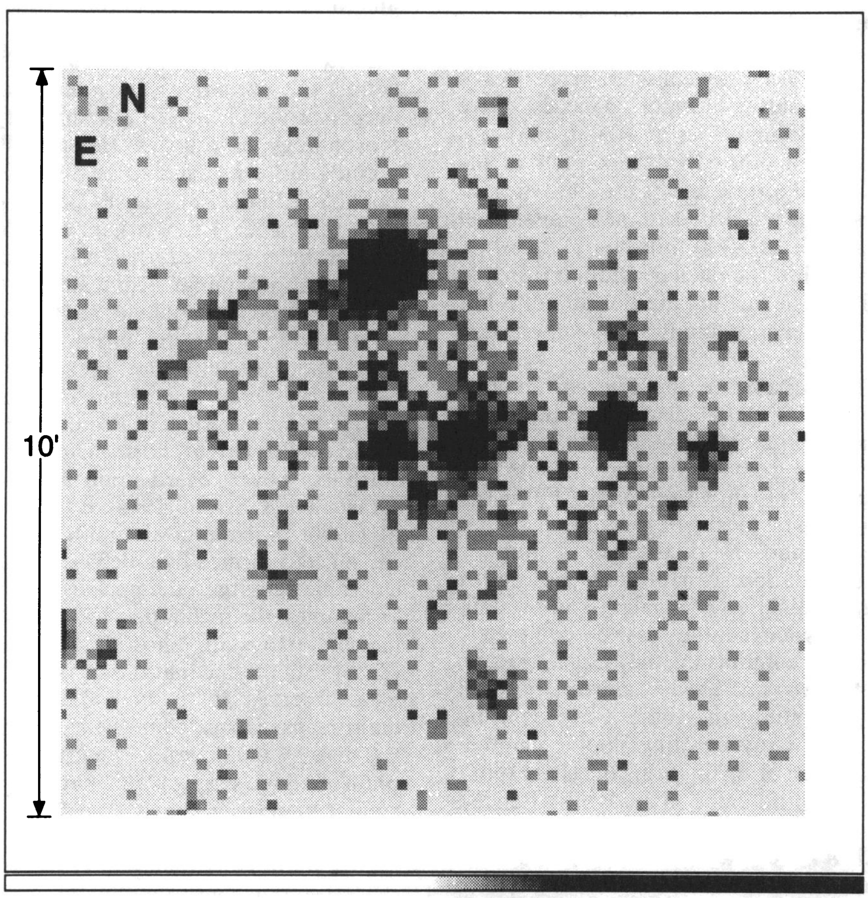

FIG. 1.—Raw PSPC photons from NGC 6946. For this and all other similar figures, north is up, east is to the left. The frame size is 10′ on a side. Each pixel is 8″ square. No background subtraction or exposure corrections have been applied at this point in the reduction. The quality of the *ROSAT* PSPC is evident without any additional work. All photons between 0.2 and 2.1 keV are shown. The number of counts in the highest pixel is 233.

in Snowden et al. (1993). No after-pulses were seen in the background spectrum (identified by an upturn in the counts distribution in moving toward the lowest channels). The background light curve showed a relatively constant count rate of ~ 5 counts s^{-1} for each *ROSAT* observation interval. The exceptions were an increase in the count rate at the end of two observation intervals (possibly due to solar scattered X-rays) and two "bursts" occurring in the middle of another two observation intervals. The detailed light curves and backgrounds of these intervals were examined for possible contamination and no compelling reason existed to eliminate any photons in these time intervals. The count rate during the "bursts" was only a factor of 2 above the nearly constant count rate during the other observation intervals. A factor of 2 is somewhat small compared to the factor of 6–8 increase cited by Snowden et al. (1994) as the result of short-term enhancements. Long-term enhancements probably also represent a small contaminant in the NGC 6946 pointing. The total observation occurred over a 5 day interval, while the long-term enhancements typically vary over 1–2 day intervals with an amplitude of $\sim 60\%$. Within the small scatter, no variation was seen in the count rate from the start to the end of the observation. The master veto rate (Snowden et al. 1992) was also examined for each observation interval. No systematic effect was seen in the image when time intervals, corresponding to slightly high master veto rates, were screened out.

3. THE OVERALL IMAGE AND THE DIFFUSE EMISSION

I turn now to the data reduction of the image as a lead into the analysis of the apparent diffuse emission. As a general note, the data were manipulated using the PROS software. The energy resolution of the *ROSAT* PSPC is approximately 40% at 1.0 keV (Pfeffermann et al. 1986), therefore, detailed spectral fits of the diffuse emission are not possible, particularly given the low number of counts observed in the diffuse emission. The spectral resolution is sufficiently good, however, that images in a few spectral bands can be produced. Table 1 lists the energy bands used in this study, as defined by Snowden et al. (1994). In this paper, I use only Snowden et al. bands R2 to R7, with Snowden et al. band R2 corresponding to my "band 1" and band R7 corresponding to "band 6." A supplementary band has been added covering channels 202–242. Although this portion of the *ROSAT* PSPC bandpass has not yet been well calibrated, it may be instructive to examine the hardest photons detectable with the PSPC. The softest photons have been ignored due to the "electronic ghost image" effect (Nousek & Lesser 1993) which is essentially a nonunique position determination. This is not a significant loss as the known column to NGC 6946 is somewhat high ($N_H \sim 5 \times 10^{21}$ cm^{-2}), so there are likely to be very few photons in this band from NGC 6946.

The photons from the galaxy were blocked by a factor of 16 and filtered using the channels listed in Table 1. An image of the galaxy was created for each band. Vignetting and exposure map corrections were applied, but these corrections were very small perturbations to the image since the farthest extent of the galaxy (to be discussed below) was less than $\sim 5'$. Background image frames of the same size as the galaxy image frame were excised north, east, south, and west of the galaxy. The centers of these background frames were a few arcminutes away from the outer edge of the galaxy. The same energy channel filters were applied to create the background frames. The background frames were exposure- and vignetting-corrected; the corrections were small because the frames were near the optical axis of the *ROSAT* mirrors. The resulting background frames were then averaged, creating an average background image for each energy band. Snowden et al. (1994) argue that the background should be modeled using their prescription. The background frames used here will include, however, all components of the X-ray background as discussed in Snowden et al. (1994). I believe the difference between modeling the background and averaging the background frames to be slight, based upon the data screening described in § 2. In addition, the goals of this paper and those of Snowden et al. differ: for their study, modeling the background was a necessity as they were interested in studying the background; here I am interested only in removing it.

The galaxy and the background frames were each smoothed using a symmetric, two-dimensional Gaussian. The point-spread function of the *ROSAT* PSPC is dependent on energy; the sharpest images are produced for photons of about 1 keV (Hasinger et al. 1992). While the PSPC point-spread function is not strictly a Gaussian, for all but the highest energies the dominant term in the functional description is Gaussian; it is a good approximation and is used here. The scale parameter of the Gaussian was set to the appropriate value based on the energy dependence of the point-spread function using the mean energy of the defined energy band. Table 1 lists the FWHM of the point-spread function used for each of these bands. Before subtracting the background images, a radial profile was constructed for each individual frame. Figure 2 shows the radial profile plots of the galaxy and the background. The radial profiles were obtained by summing all counts in annuli 1.5 pixels wide, dividing by the number of pixels in the annulus, and converting the resulting number to counts $arcmin^{-2}$. The annuli were extended to 400″ from the galaxy's nucleus. The radial plots show that, beyond about 260″–300″, any galaxy emission is dominated by the background. (The "wavy" profiles in several of the plots result from some "splotchiness" in the background frames. This splotchiness may be extremely weak point sources; however, the "detect" routines do not uncover them. Within the errors, the background profiles are constant.) This exercise has the purpose of checking that the background frames have the same flux as the galaxy frames beyond the galaxy's outer edge. The radial profiles in Figure 2 show this is indeed the case. The background fames can then be subtracted from the source plus background frames without further scaling. The north arm source clearly dominates the profile plots in all bands. (Further discussion of the radial profiles is deferred to § 5.) The results of the band-by-band subtraction are displayed in Figure 3. Figure 3*a* shows the image of the galaxy scaled to a common value for

TABLE 1

ENERGY CHANNEL DEFINITIONS AND FWHM OF THE POINT-SPREAD FUNCTION

Band	Channels	Energy Range (keV)	Mean Energy	FWHM	σ (pixels)
1.........	20–41	0.20–0.41	0.28	42″2	2.2
2.........	42–51	0.42–0.51	0.47	36.2	1.9
3.........	52–69	0.52–0.70	0.61	33.2	1.8
4.........	70–90	0.70–0.90	0.80	29.8	1.6
5.........	91–131	0.91–1.32	1.10	26.4	1.4
6.........	132–201	1.32–2.02	1.67	33.0	1.75
7.........	202–242	2.02–2.45	2.20	134.4	7.1

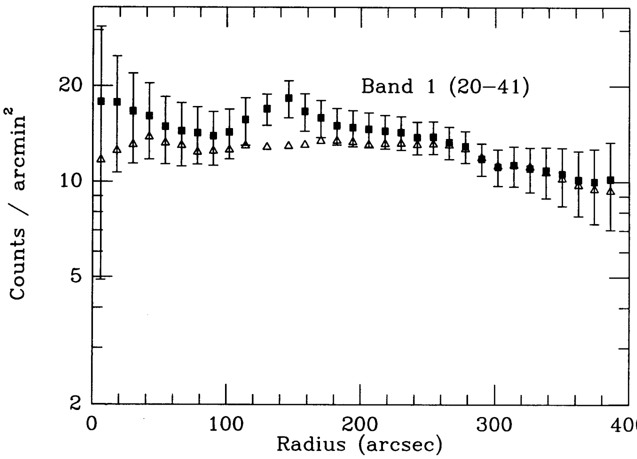

FIG. 2*a*

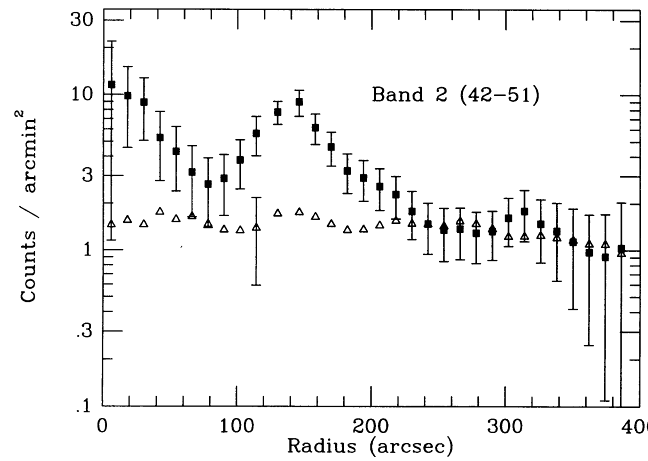

FIG. 2*b*

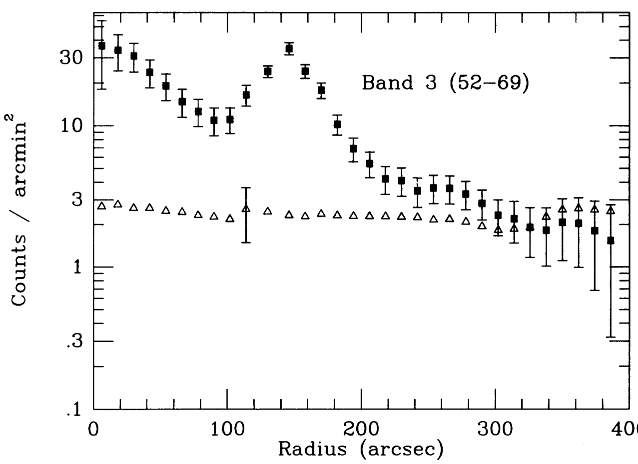

FIG. 2*c*

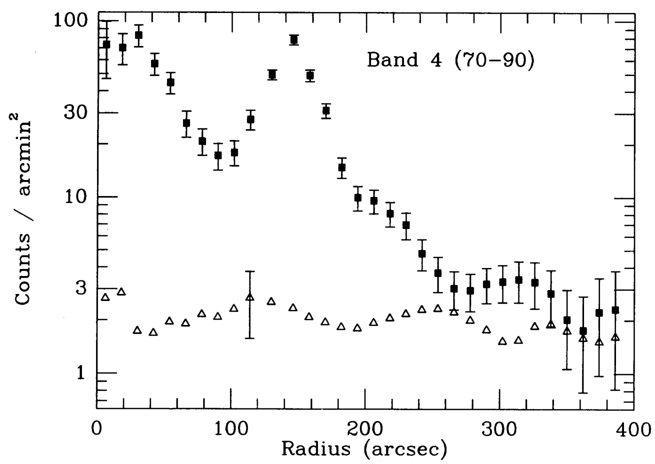

FIG. 2*d*

FIG. 2.—(*a*)–(*g*) Radial profile plots of NGC 6946. The radial bins are 1.5 pixels wide (12″). The plots are labeled by the energy band and channel numbers corresponding to the entries in Table 1. Only a representative error bar has been included for the background profiles for clarity. It is clear that the galaxy is ~300″ in radius.

all frames. Figure 3*b* shows the images normalized frame by frame, bringing out the weaker structure in each image. Together, Figures 3*a* and 3*b* are equivalent to a hardness map of the galaxy in which a different color is assigned to each band. Figure 4 shows the image obtained by summing the individual bands to obtain the final, background-subtracted image.

Figure 5 shows the contoured version of Figure 4 overlaid on an optical reproduction of the Palomar Sky Survey (red plate). The optical pixels are 1″.7 in size. The optical galaxy has a size of about 6′–7′, comparable to the X-ray image. The X-ray contours start at 0.3% of the peak, with additional contours at 0.5%, 1%, 3%, 5%, 10%, 30%, and 50%. The peak flux in the smoothed image is 98 counts. The X-ray contours generally follow the galaxy's optical morphology; specifically, the contours follow the bright northeastern spiral arm, as well as the eastern and western arms. These three arms are the most developed arms in NGC 6946. X-ray emission from the north arm is completely dominated by the north arm source. In the southwestern portion of the galaxy the situation is somewhat confused because it is not apparent exactly which arms join at what point on the nucleus. Note that the X-ray emission generally appears to remain within the bright optical image, except, perhaps, on the western side of the galaxy. This region also appears to be dominated by weak sources, so the contours may be biased by these sources.

The counts in the diffuse emission can be extracted and a spectral fit done, even if the fit is poor. The extraction region used was a polygon shaped approximately as a rectangle oriented with the long axis parallel to the major axis of the galaxy. This region was a compromise between a huge region that included X-rays not clearly from NGC 6946 and a region too small to include the obvious extent of the galaxy. The coordinates of the nodes of the polygon are listed in the notes to Table 2. The spectral fitting results are included in Table 3 with the individual sources (§ 4 below). None of the fits is preferred over any of the others. The arbitrarily chosen spectrum presented in Figure 6*a* is the thermal bremsstrahlung spectrum. A systematic error of 2% was added to each channel for all spectra. This systematic error masks the known problems with the response matrix. The contour plot of N_H versus kT is shown in Figure 6*b*. (In this paper, all contour plots show the $\Delta\chi^2$ levels of 2.71 (90% for one parameter of interest), 4.61 (90% for two parameters of interest), and 9.21 (99% for two

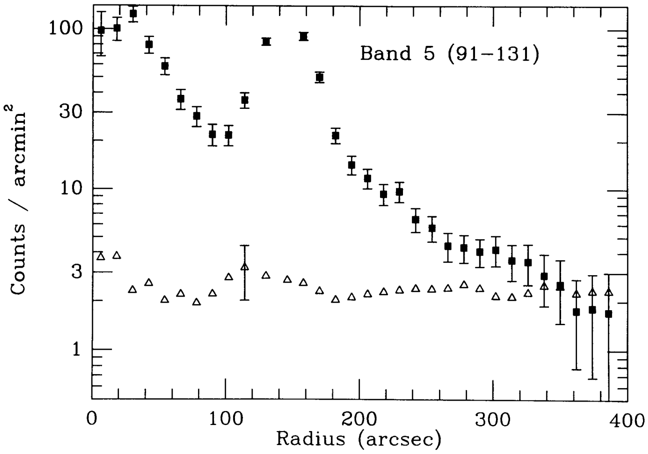

FIG. 2*e*

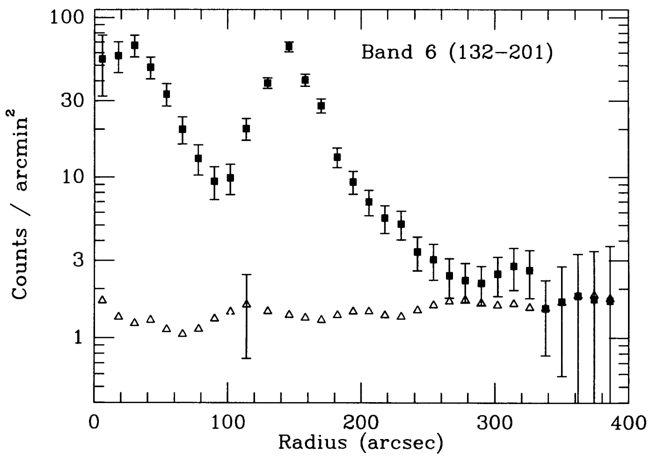

FIG. 2*f*

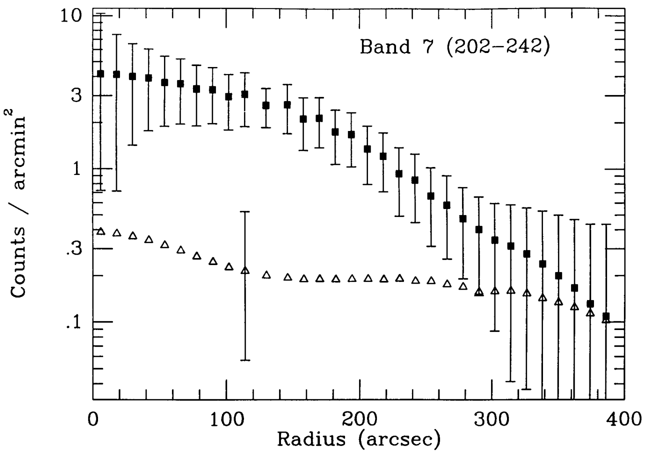

FIG. 2*g*

parameters of interest. The reader should pay most attention to the outer two contour levels.) The fitted temperature is soft with $kT \sim 0.5$ keV. The fitted column is $\sim 3 \times 10^{21}$ cm^{-2}, which is somewhat low relative to the known column of $\sim 5 \times 10^{21}$ cm^{-2} (Burstein & Heiles 1984), but within the uncertainties the two values can be considered equal. The 0.5–2.0 keV luminosity is $\sim 3.8 \times 10^{36}$ ergs s^{-1} arcmin^{-2} or $\sim 9.4 \times 10^{38}$ ergs s^{-1} over the polygon aperture (essentially the entire galaxy).

Wang et al. (1991) and Trümper et al. (1991) have recently demonstrated the existence of a very hot component of the ISM in the Milky Way and the LMC. This component, with a temperature of $10^{6.2}$–10^7 K, probably represents the direct input of supernova heating. Whether the hot component is a major constituent of the ISM is still debated (i.e., is the filling factor 1%, 10%, or more?), although *ROSAT* observations may establish the case one way or the other. A crude estimate

TABLE 2

SOURCES IN THE NGC 6946 FIELD

Source	R.A. (2000)	Decl. (2000)	Aperture[a]	Counts	S/N	Hardness[b]	Approximate Flux[c] (ergs s^{-1} cm^{-2})	Luminosity[c] (ergs s^{-1})
S1[d]	20^{h}35^{m}01^s	60°11′32″	0′.70	2326.4 ± 46.8	32.1	+0.28	8.3 ± 0.2 (−13)	3.0 ± 0.1 (39)
S2	20 34 37	60 09 34	0.70	169.9 ± 12.9	7.7	+0.26	6.0 ± 0.5 (−14)	2.2 ± 0.2 (38)
S3	20 34 52	60 09 14	0.70	219.6 ± 15.7	8.5	+0.36	7.9 ± 0.7 (−14)	2.8 ± 0.3 (38)
S4	20 35 01	60 09 09	0.70	153.9 ± 12.7	6.9	+0.11	5.5 ± 0.5 (−14)	1.9 ± 0.2 (38)
S5	20 34 49	60 12 21	0.70	43.4 ± 6.5	3.9	+0.81	1.5 ± 0.3 (−14)	5.5 ± 0.6 (37)
S6	20 34 57	60 08 30	0.70	55.2 ± 6.9	3.8	+0.21	1.9 ± 0.3 (−14)	6.8 ± 1.1 (37)
S7	20 35 01	60 10 09	0.46	61.6 ± 9.7	4.1	+0.42	2.2 ± 0.4 (−14)	7.9 ± 1.5 (37)
S8	20 34 26	60 09 15	0.70	58.9 ± 6.8	4.1	+0.86	2.1 ± 0.2 (−14)	7.6 ± 0.7 (37)
S9	20 34 49	60 05 57	0.70	51.9 ± 8.1	4.2	+0.64	1.8 ± 0.3 (−14)	6.5 ± 1.2 (37)
Diffuse[e]	...	...	8.72	931.6 ± 45.3	18.5	−0.03	2.6 ± 0.3 (−13)	9.4 ± 0.1 (38)
Bkgrd[f]	...	...	16.8	1513.4 ± 38.4	38.5	−0.51	5.4 ± 0.3 (−13)	...

[a] Aperture radius. Approximately 90% of each source is enclosed in the aperture except for source S7. Source crowding forced the use of a smaller aperture enclosing ~62% of the flux.

[b] Hardness ratio, defined in § 4.

[c] Numbers in parentheses are exponents. The counts and fluxes have been corrected for the flux outside the aperture. The energy range over which the flux and luminosity were calculated is 0.5–2.0 keV.

[d] Source described in detail by Schlegel 1994a.

[e] "Diffuse" emission represents the entire galaxy minus the point sources S1–S9. The aperture used was a polygon, so the aperture "size" is the circle of equal area. The polygon's nodes are at (1) 20^{h}34^{m}58^s, 60°13′09″; (2) 20^{h}35^{m}27^s, 60°10′39″; (3) 20^{h}35^{m}14^s, 60°08′07″; (4) 20^{h}34^{m}49^s, 60°05′25″; (5) 20^{h}34^{m}30^s, 60°07′15″; and (6) 20^{h}34^{m}20^s, 60°09′23″. This polygon essentially surrounds the optical image of the galaxy.

[f] "Bkgrd" represents the background emission in an annulus surrounding the entire galaxy minus any point sources. The aperture used was a polygonal annulus, so the aperture "size" is the radius of the circle of equal area. The polygon's outer nodes are at (1) 20^{h}34^{m}54^s, 60°15′17″; (2) 20^{h}35^{m}46^s, 60°10′51″; (3) 20^{h}34^{m}45^s, 60°02′50″; and (4) 20^{h}33^{m}52^s, 60°09′33″. The inner boundary of the background region was the outer boundary of the diffuse emission.

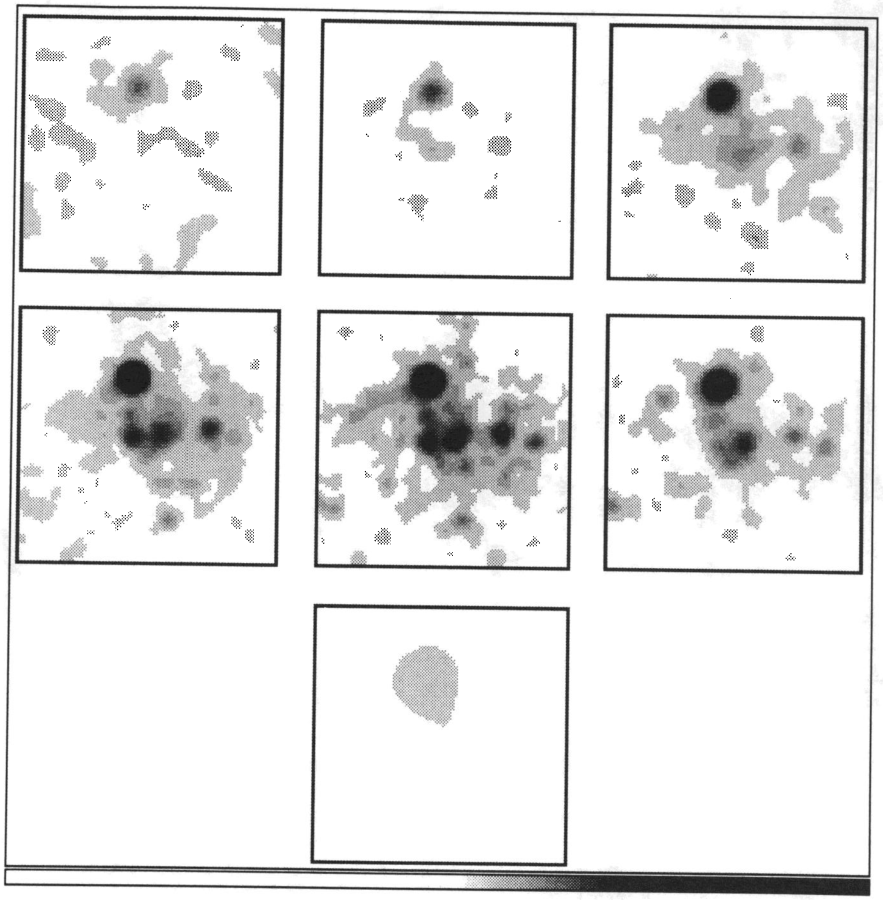

FIG. 3a

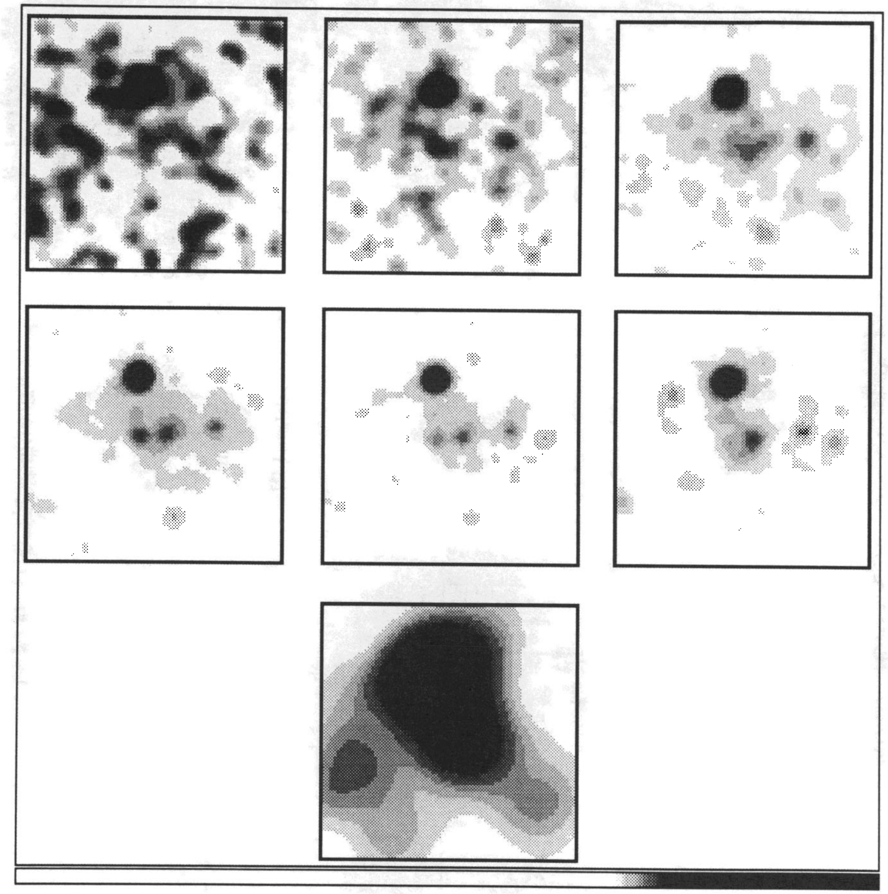

FIG. 3b

FIG. 3.—Scaled images of NGC 6946 by energy band. The bands run from left to right, top to bottom, so the lowest-energy band is in the upper left corner. Each pixel is 8″ square, so the frames are 10′ on a side. The background corresponding to each band has been subtracted. The images have been smoothed as described in § 3 of the text. The image arrays differ only by the scaling: (*a*) one value scales all the images; (*b*) all images are scaled individually.

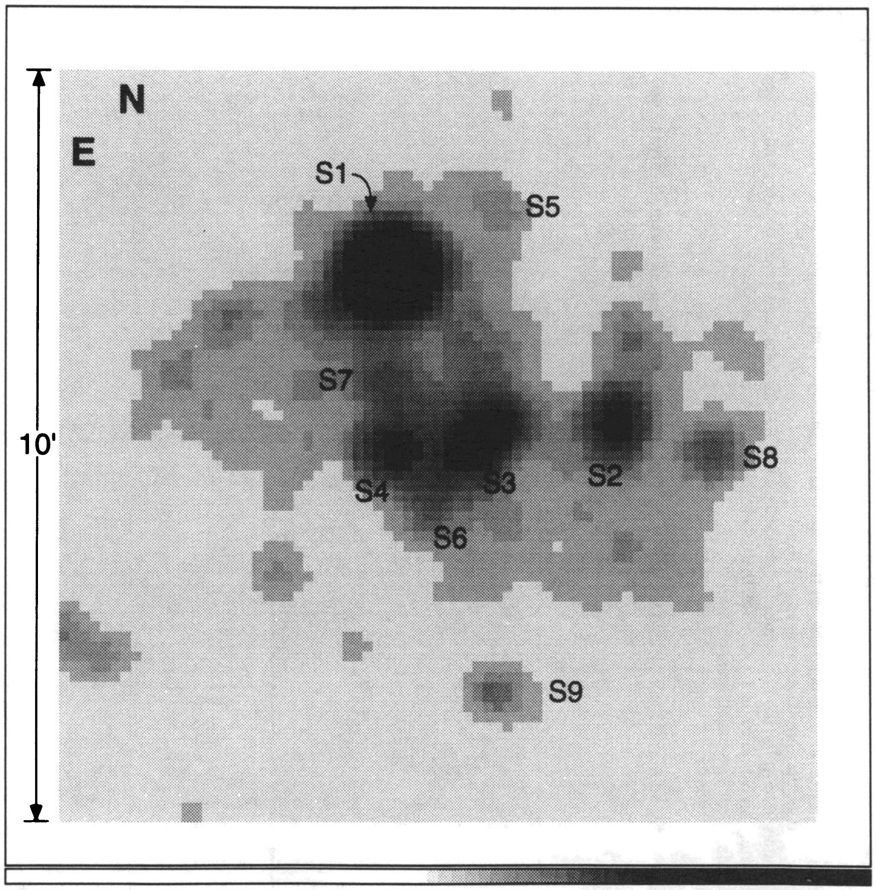

FIG. 4

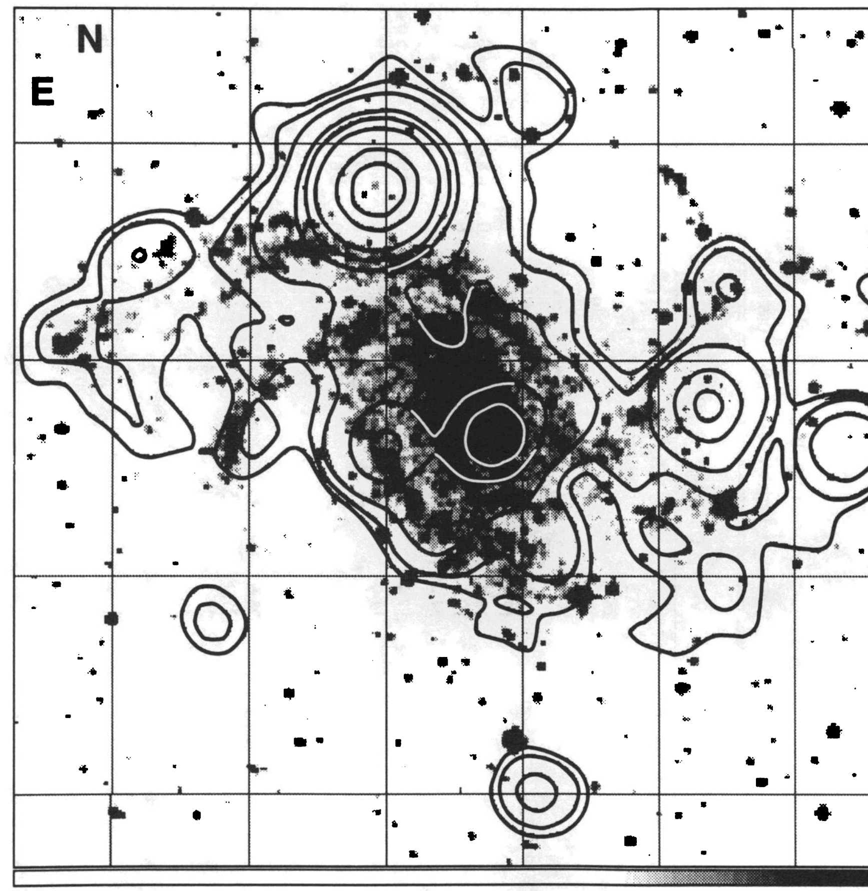

FIG. 5

FIG. 4.—Summed, background-subtracted image of NGC 6946 from Fig. 3*a*
FIG. 5.—Contour plot of Fig. 4 overlaid on an optical (red) image of NGC 6946

TABLE 3

SPECTRAL FITS TO STRONG SOURCES

Source	Counts	Model[a]	χ^2	Channels[b]	N_H (10^{22} cm^{-2})	90% Error Range[c]	kT (keV) or α	Approximately 1 σ Error Range[c]
S1[d]	2326.4 ± 46.8	Power	28.1	33	0.61	0.49–0.73	4.9	4.2 –5.6
		Blackbody	30.2	33	0.17	0.11–0.23	0.24	0.22–0.26
		Brems	28.9	33	0.35	0.30–0.43	0.48	0.37–0.59
		Mewe	27.2	33	0.37	0.31–0.42	0.46	0.42–0.50
		Brems-F	38.7	33	0.50F	...	0.37	0.33–0.40
2	169.9 ± 12.9	Power	18.1	25	0.88	0.56–1.20	7.86	5.86–9.80
		Blackbody	17.9	25	0.05	0.03–0.07	0.21	0.19–0.23
		Brems	19.8	25	0.31	0.16–0.87	0.33	0.17–0.53
		Mewe	19.6	25	0.42	0.13–0.73	0.31	0.18–0.44
		Brems-F	34.2	25	0.50F	...	0.33	0.29–0.37
3	219.6 ± 15.7	Power	17.4	27	0.73	0.48–0.98	5.09	3.65–6.53
		Blackbody	17.6	27	0.28	0.14–0.42	0.23	0.19–0.27
		Brems	17.3	27	0.47	0.31–0.71	0.45	0.29–0.81
		Mewe	17.6	27	0.47	0.33–0.61	0.44	0.36–0.52
		Brems-F	17.5	27	0.50F	...	0.54	0.38–0.67
4	153.9 ± 12.7	Power	24.5	23	1.00	0.65–1.35	8.80	6.60–11.0
		Blackbody	25.6	23	0.27	0.11–0.43	0.15	0.12–0.19
		Brems	27.3	23	0.32	0.20 0.64	0.30	0.19–0.38
		Mewe	27.3	23	0.42	0.06–0.76	0.30	0.16–0.47
		Brems-F	40.5	23	0.50F	...	0.31	0.27–0.34
Diffuse[e]	931.6 ± 45.3	Power	12.2	28	0.29	0.09–0.59	4.28	3.01–5.56
		Blackbody	13.1	28	0.05	0.02–0.10	0.21	0.18–0.23
		Brems	12.2	28	0.11	0.07–0.21	0.56	0.10–0.91
		Mewe	11.9	28	0.08	0.07–0.23	0.54	0.38–0.64
		Brems-F	18.8	28	0.50F	...	0.21	0.11–0.38
Weak[f]	271.1 ± 17.2	Power	3.9	14	1.33	...	4.98	...
		Blackbody	2.9	14	0.05	...	1.01	...
		Brems	2.0	14	0.69	...	0.99	...
		Mewe	2.6	14	0.95	...	0.51	...
		Brems-F	2.2	14	0.50F	...	1.55	...

[a] The number of free parameters is three for all models except the fixed bremsstahlung model (designated "Brems-F"), in which the column N_H is held fixed at 0.5×10^{22} cm^{-2}. For the Mewe models, the abundance is fixed at 1.0.

[b] The number of binned channels used in the fit. The number of extracted channels was identical for all sources and covered the full energy range of the PSPC (0.1–2.4 keV). Due to the moderately high column to NGC 6946, there were few photons below ~0.3 keV.

[c] The error ranges were calculated for two parameters of interest.

[d] Source S1 is described in Schlegel 1994a.

[e] See note e in Table 2.

[f] "Weak" represents the sum of the sources S5–S9. Due to the generally poor statistics, error ranges are uniformly large and are not quoted.

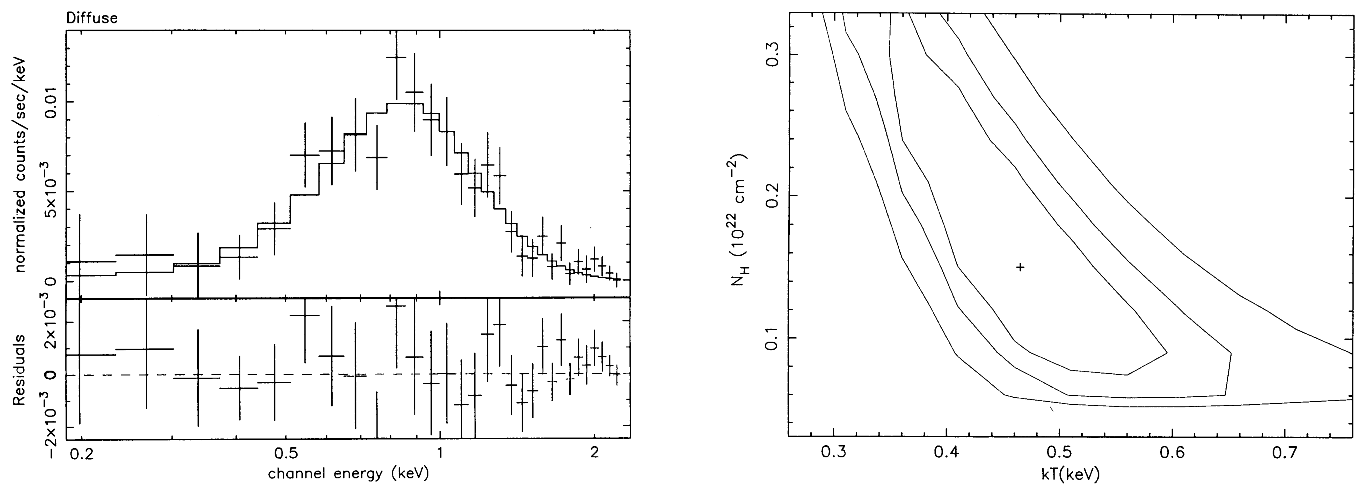

FIG. 6a FIG. 6b

FIG. 6.—Extracted spectrum (*a*) and contour plot (*b*) of the diffuse emission. The extraction aperture was a polygon surrounding the galaxy with circles excluding the point sources.

can be made of the number density from the diffuse emission luminosity. The estimate comes from

$$L_X \sim \Lambda n_e^2 V ,$$

where Λ is the plasma cooling function. Wang, Hamilton, & Helfand (1989) plot the cooling function for various values of the column density. The value most appropriate to the PSPC data of NGC 6946 is $\Lambda \sim 5 \times 10^{-24}$ ergs cm^3 s^{-1}, ignoring for now possible abundance differences. The volume of NGC 6946 can be approximated as a flat cylinder of radius $\sim$14 kpc and thickness h. These values then yield $n_e^2 hf \sim 10^{-2}$ cm^{-6} pc, where f is the volume filling factor. For $h \sim 100$ pc and $f \sim 0.1$, $n_e \sim 0.1$ cm^{-3}. This value is comparable to the hot ISM component of the LMC (e.g., Wang 1993; Wang et al. 1991) and suggests that the diffuse emission in NGC 6946 is that galaxy's hot ISM. I shall discuss the diffuse emission again in the context of whether the emission is the sum of unresolved point sources.

4. POINT SOURCES

The *ROSAT* PSPC data on NGC 6946 impressively resolves the X-ray emission, formerly attributed to the nucleus by the *Einstein* IPC study, into nine sources. Figure 4 shows the source positions. These sources all have a signal-to-noise ratio greater than 3.5 as generated by the PROS detect tasks. The background region used is the entire galaxy from § 3. This may overestimate the local background at a particular source as the diffuse X-ray emission is not uniform. Absolute positions (α, δ) were derived from the raw positions by adding the corrections $\Delta\alpha = 1\overset{s}{.}6$, $\Delta\delta = -6\overset{''}{.}4$. These corrections were obtained by comparing the PSPC positions of two known *Einstein* sources and one HD star with their catalog positions. While three sources are not a large statistical sample, these three objects are the only point sources in the NGC 6946 pointing which have clear identifications, thereby minimizing source confusion. Table 2 lists the individual sources with entries for the R.A. and Decl., the extraction aperture size, the counts obtained, the signal-to-noise ratio, the hardness ratio [defined as $(H-S)/(H+S)$, where S = channels 20–90 = 0.2–0.9 keV and H = channels 91–201 = 0.9–2.0 keV], and the approximate flux and luminosity. Fluxes were calculated assuming a thermal bremsstrahlung spectrum of $kT = 1$ keV plus the galactic column to NGC 6946 (Burstein & Heiles 1984). The derived fluxes are insensitive to the exact spectral model due to the large uncertainties resulting from the low count rate. Table 3 lists the spectral fits to the individual sources with sufficient counts, including, as a "source," the diffuse emission described above and a spectrum obtained by summing all of the weak sources. The number of extragalactic sources present in the immediate NGC 6946 region is expected to be less than 1 based on the log N–log S relation from the *ROSAT* medium-sensitivity survey (Hasinger, Schmidt, & Trümper 1991). In addition, the fitted column for all sources is relatively high (a few $\times$ 10^{21} cm^{-2}). On this basis, I believe all the sources listed in Table 2 are local to NGC 6946. The brightest source, S1 lies near the north arm of the galaxy and is the "north arm" source discovered in the IPC data (FT). The luminosity of the source is $\sim 3 \times 10^{39}$ ergs s^{-1}, which is unchanged within the errors from the value quoted by FT. This source has been identified as a supernova remnant (Schlegel 1994a; Blair & Fesen 1994) and will not be discussed any further in this paper.

Of the remaining sources, only S2, S3, and S4 individually provide sufficient statistics to attempt crude spectral fitting. The spectral fits are listed in Table 3, while the spectra and $N_{\rm H}$ versus kT contours are displayed in Figure 7. The thermal bremsstrahlung spectrum is used as the default spectrum for the displayed spectra. The abundances for the Mewe models were fixed at solar values. Sources S2 and S4 are relatively soft, with thermal bremsstrahlung temperatures $kT \sim 0.5$ keV. The temperature of source S3 is essentially indeterminate. On the basis of $\Delta\chi^2$, no particular model is preferred to any other. All of the power-law models, however, yield values for $N_{\rm H}$ considerably higher than the known galactic column, so these models may not be the best match to the data, although the reader should note that galactic sources do exist with intrinsically high $N_{\rm H}$. The blackbody models tend to produce an $N_{\rm H}$-value quite low relative to the known column; the believability of these models should be somewhat lower. While source S4 shows evidence for a slightly lower temperature, the χ^2 contours of all three sources overlap at the 99% level. Optical follow-up studies are planned at least for sources S2 and S4, both of which have sufficient counts to obtain a reasonably accurate position.

The remaining sources (S5–S9) only have count rates and hardness ratios available. Based upon the hardness ratios, most of the sources are relatively soft [$(H-S)/(H+S) \sim 0.3$–0.5]. Sources S5 and S8 are relatively harder, which suggests the possibility that they may be X-ray binaries, although the PSPC energy band is sufficiently narrow that this possibility should be read as a hint rather than a conclusion. The emission of the weaker sources can be summed and a spectral fit done. The statistics are rather poor due to the low count rates of the few weak sources. The contour plot is shown in Figure 7; the fitted spectrum was deemed not worth presenting as it appears as a noisier version of the spectra already present. A comparison of the contour plots of the diffuse emission (Fig. 6*b*) and the summed weak sources shows that the summed weak sources have a higher temperature than the diffuse emission. The evidence is not overwhelming, but the contours are essentially mutually exclusive at about the 95% level. The summed weak source contours extend to much higher temperatures (the fit does little more than establish a lower limit to the temperature of $\sim$0.5–1 keV), while the contours of the diffuse emission are confined rather tightly below $\sim$0.7 keV. The fitted column for the weak sources provide a hint that these objects may lie within the plane due to its higher fitted value. The reader should note the size of the contours, however. These hints about the differences between the diffuse emission and the weak sources may be more easily seen by examining the hardness ratios for each (Table 2). Finally, the positions of the remaining sources (S5–S9) may not be sufficiently well determined to produce a sufficiently small error circle that would make an optical follow-up useful. Source S9 is well separated from the galaxy itself and may have sufficient counts to determine an accurate position, largely as a result of the lower galactic background at that location.

The PSPC image can also be used to look for 0.5–2.0 keV emission from sources identified in other wavelength bands. The original motivation to obtain a PSPC image of NGC 6946 was the study of the historical supernovae which have occurred in this galaxy. SN 1980K is almost certainly present; SN 1968D may be visible. Both are weak sources. The other four historical supernovae are not visible in the PSPC data. The complete description of these results is presented in Schlegel (1994b). Klein et al. (1982) list sources they found in their radio survey of NGC 6946. The positions listed in their Table 2 were

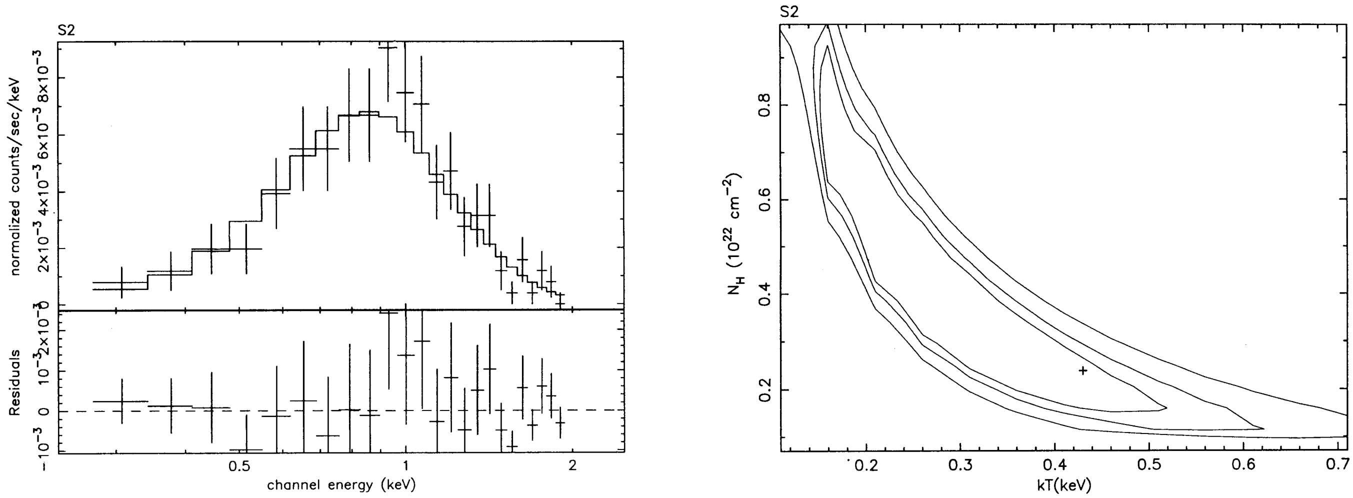

FIG. 7*a*

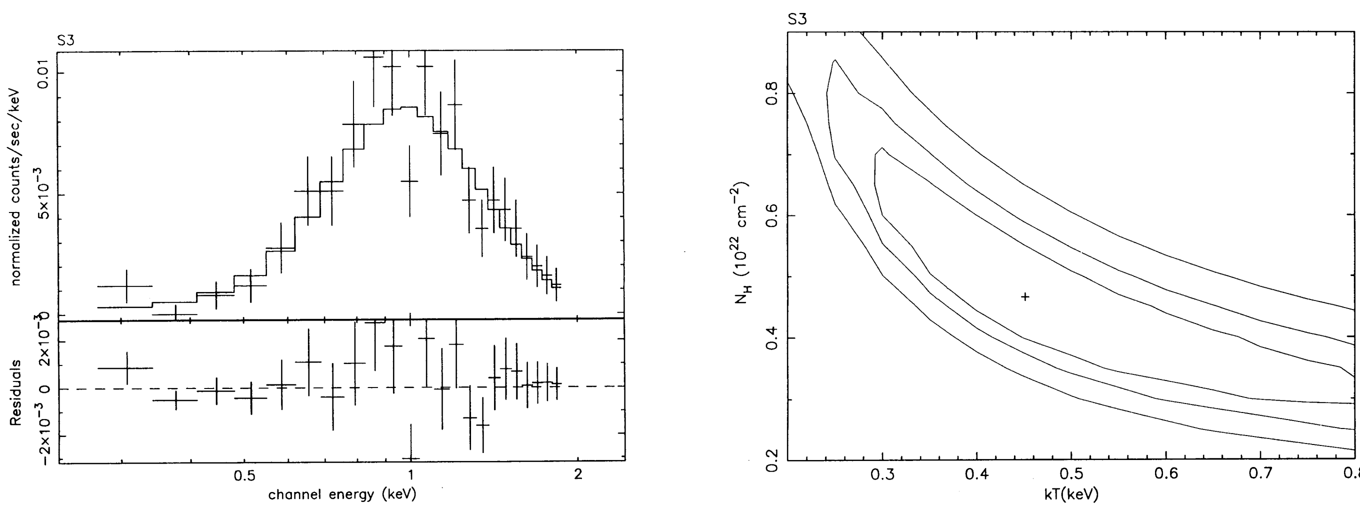

FIG. 7*b*

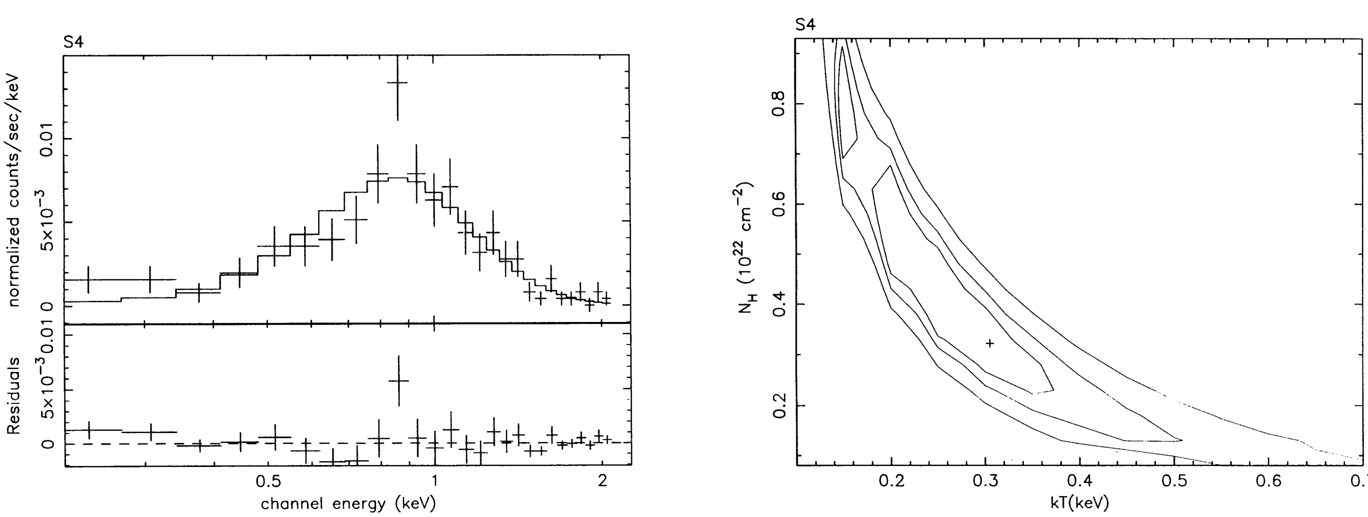

FIG. 7*c*

FIG. 7.—Extracted spectra (*left panels*) and contour plots (*right panels*) of the relatively bright, individual sources (*a*) S2, (*b*) S3, (*c*) S4, and (*d*) the summed emission of the weak sources S5–S9. Only a contour plot is included for the summed weak sources. The equivalent plots for source S1 are included in Schlegel (1994a).

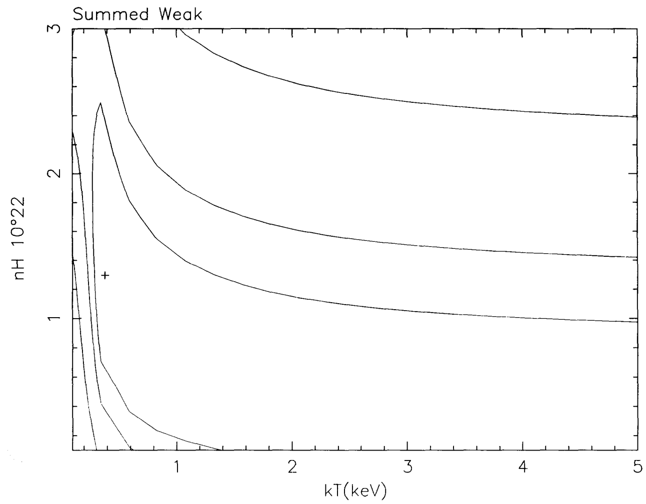

FIG. 7*d*

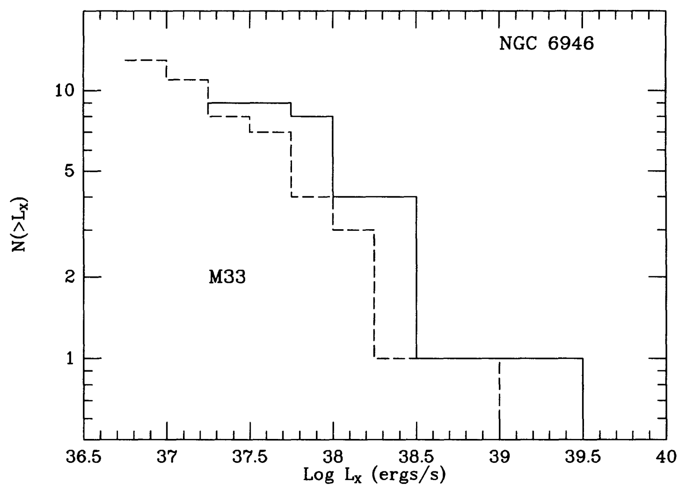

FIG. 8.—Integrated number distribution of sources in NGC 6946 compared to the *Einstein* IPC data on M33 (Trinchieri et al. 1988).

converted to J2000 and overplotted on the X-ray image. No match exists of any of the radio sources with the PSPC sources except for the nuclear source (Klein et al. 1982, source A). Source A of Klein et al. corresponds, within the positional accuracy, to source S3 in this paper. From the PSPC spectrum, S3 shows no apparent discrepancy in the column from the galactic value. This is somewhat surprising as many studies of galaxies discuss the internal extinction in the nucleus and derive high upper limits or measurements of a large extinction (see, e.g., Trinchieri et al. 1985). Engargiola (1991) and Devereaux & Young (1993) showd from their far-IR studies that dust absorption is very high in the central 5′. One might expect the hydrogen column to show similar behavior. Since *ROSAT* is quite sensitive to soft photons, which are easily absorbed, one expects a good estimate for the total column from the spectral fits. For NGC 6946, DeGioia-Eastwood et al. (1984), Engargiola (1991), and Devereaux & Young (1993) all derive a nuclear A_V of ~ 2. This value corresponds to an N_H of $\sim 5 \times 10^{21}$ cm^{-2}. The spectral-fitted N_H is consistent, within the errors, with that value. Note also that NGC 6946 is a low-power starburst galaxy (Telesco & Harper 1980; Giuricin et al. 1991). No apparent spectral signature appears in the *ROSAT* band. However, the lack of a starburst signature has been noted, for example, in M83 (Trinchieri et al. 1985) in which the ratio of X-ray to optical flux was not found to be enhanced as might be expected of star-forming galaxies. Fabbiano, Feigelson, & Zamorani (1982) concluded from their peculiar galaxy study that nuclear emission does not dominate the X-ray emission of a galaxy like NGC 6946.

Before leaving the discussion of the nucleus, note that the image of the nucleus appears slightly elongated in the northwest-southeast directions. Since source S1 is quite circular in appearance, a poor aspect solution is ruled out as an explanation. The elongation can be quantified to some degree by comparing the counts in annuli, in wedges oriented along the major and minor axes. Due to the few counts in the source, the result is rather noisy, but an elongation of about 1.5:1 is suggested for the major to the minor axis. There are too few counts to attempt to deconvolve a composite source. Further work may be justified if a detailed understanding of the point-spread function becomes available. If we assume the source is two sources radiating at half the rate, then a 10 ks *ROSAT* high-resolution imager (HRI) observation should yield a 4–5 σ detection of each source, making the issue an observational question.

Figure 8 shows the integrated number distribution for the NGC 6946 sources (*solid line*). For a comparison, the *Einstein* IPC data on M33 have been used (Trinchieri et al. 1988). M33 is a face-on Sc galaxy, so the comparison has been deemed appropriate. In addition, the *ROSAT* PSPC data reach to approximately the same flux level as the IPC data on M33. The IPC data uncovered 13 sources definitely attributed to M33. The distributions for the two galaxies are nearly identical over most of the luminosity range. Admittedly, both distributions are examples of small-number statistics. If source S1 did not exist, however, the two distributions would most likely be used to illustrate the overall similarity of the source distribution present in spiral galaxies or, at least, in Sc–Scd galaxies.

Finally, the brightest sources were examined for possible time variability. Timing with the *ROSAT* PSPC is problematic except for very short times (of order milliseconds) or very long times (of order hours to days). A period search was done on sources S1, S2, S3, and S4 using the PROS task "period," which permits a range of periods to be examined and calculates a χ^2 value for each period. Ten bins were used per period and periods from 10 msec to 10 s were examined with a time resolution of $\sim 5\%$ of the period. For this type of search, χ^2 should have a value approximately equal to the number of bins used. Any value greatly exceeding the expected mean was then examined in greater detail with a time resolution of $\sim 1\%$. No convincing periods were seen for any of the sources over these short times. The longer periods were examined by averaging the counts in an observational interval and comparing the average rate to the rates from the other observational intervals. Again no convincing variation was found. This approach to the time data is not ideal. It clearly avoids, however, the window and aliasing problems present due to the observation intervals and the satellite wobble.

5. DISCUSSION

I first discuss the point sources. The north arm source has apparently been constant in flux, within the errors over the intervening ~ 12 yr (Schlegel 1994a). The source clearly is localized to the northern arm of the galaxy, but is *not* coincident with the Klein et al. (1982) source, as suggested by FT. The better X-ray positional resolution of the PSPC clearly places the Klein et al. radio source several arcminutes east of the X-ray source (VanDyk et al. 1994). Ironically, the X-ray source does not lie on the optically prominent northeastern arm. The nucleus seen with the IPC is now resolved into at least three sources, two of which are relatively prominent. Both happen to be somewhat soft, thus explaining FT's result of a softer spectral fit for the total NGC 6946 IPC spectrum.

If we take the spectral fits and hardness ratios at face value, however, then sources S2, S4, and S6 may be supernova remnants, while sources S5, S8, and S9 may be X-ray binaries. Sources S3 and S7 are probably not cleanly enough separated by the hardness ratio to identify them. If this crude form of identification were to hold, and including source S1, then the high end of the X-ray–emitting luminosity function of NGC 6946 would be dominated by supernova remnants. This may not be surprising if NGC 6946 is a moderate starburst galaxy. Thus, if the identifications are at all reasonable, *ROSAT* can be expected to uncover a sizable population of supernova remnants in the nearby galaxies. Some support for this result is provided by the M33 PSPC image (Long et al. 1994) in which many of the detected sources are known remnants. Perhaps the overall population of soft sources in NGC 6946 is an evolutionary quirk, in that the harder sources are slightly fewer in number. I must also include, however, the caution that the PSPC has a very soft response, so it is somewhat insensitive to a hard spectrum. Only a classwide study of Sc galaxies observed with the PSPC will address this issue. Such a study will not be possible for at least a few years, or until the *ROSAT* archive becomes populated with sufficient pointings to provide a reasonable number of galaxies.

Is the diffuse emission the sum of unresolved point sources? For NGC 6946, the diffuse emission has a hardness ratio considerably different from the ratios of any of the point sources. The contours of the spectral fit suggests that the diffuse emission is not the summed emission of sources similar to the weak detected sources. The $N(>L_X)$–L_X relation can be extrapolated to lower L_X to see if the diffuse emission is consistent with the emission of unresolved sources. Such an extrapolation implies approximately 12 sources with L_X of $\sim 5 \times 10^{36}$ ergs s^{-1} and ~ 20 sources with L_X of $\sim 1 \times 10^{36}$ ergs s^{-1}. This represents about a factor of 5 too little luminosity to account for the diffuse emission. From an alternative point of view, the discussion in Primini, Forman, & Jones (1993) on the diffuse emission in the central region of M31 can be followed. In their paper they list the possible sources, the size of the source population, and the typical X-ray luminosity. They then show that no particular population can account for the diffuse emission in the central region of M31. For example, one can quickly show that cataclysmic variables do not have sufficient numbers to account for more than a few percent of the diffuse emission. The same analysis can be applied to NGC 6946 with suitable adjustments to account for the differences between the central region population of Primini et al. and the disk population of NGC 6946. That exercise leads to the same conclusion: the diffuse emission cannot be represented by known, unresolved point sources.

A good correlation exists for a galaxy's X-ray luminosity and its blue optical luminosity, radio luminosity, and far-IR luminosity (Fabbiano et al. 1988). The X-ray/far-IR luminosity correlation appears to be the strongest, indicating an apparent close relationship between star formation regions

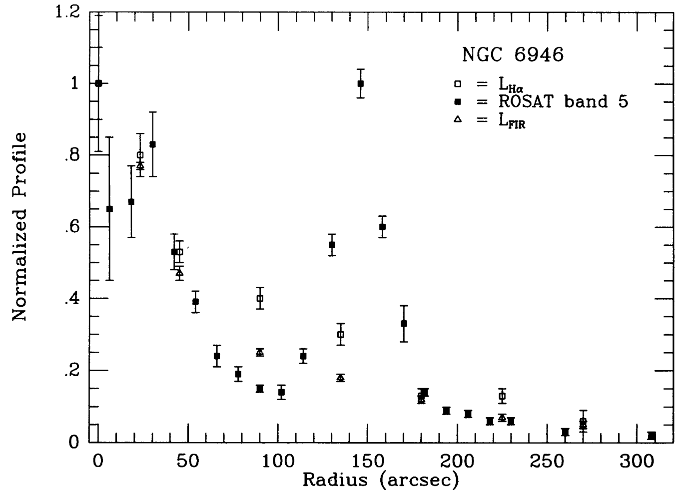

FIG. 9.—Azimuthally averaged radial distributions of the far-IR, Hα, and *ROSAT* data from band 5. Note that each radial distribution has been normalized to its own peak.

and the X-ray sources (Devereaux & Young 1993). Figure 9 shows azimuthally averaged radial distributions from the band 5 *ROSAT* data, Hα, and the far-IR (Devereaux & Young 1993). Each distribution has been normalized to its own maximum, so the absolute values cannot be compared. Overall, each of the distributions behaves in roughly a similar manner. Note, however, that the comparison may be suspect, in that the X-ray azimuthally averaged distribution is dominated by point sources (the "spike" at $\sim 150''$ is source S1), the impact of which on the radial distribution is determined by the point-spread function. The far-IR distribution is almost certainly not dominated by point sources. The Hα distribution, on the other hand, is likely the sum of H II regions. A better comparison should be possible once the point-spread function is known in greater detail, or after a deep HRI pointing has been obtained. The proper analysis would compare maps of NGC 6946 at various wavelengths; such a study is beyond the scope of the present paper.

Beck (1991) and Ehle & Beck (1993), as well as Klein et al. (1982), analyzed polarimetry data and revealed a minimum in the polarization in the southwestern (SW) quadrant where the spiral structure is least apparent. Ehle & Beck argue that the minimum suggests the galactic equivalent of a "solar coronal hole" exists. They also show that a thick disk of ionized gas is not consistent with their observations and suggest a disk thickness of ~ 100 pc is appropriate and argue that the magnetic field is perpendicular to the plane of the galaxy in the SW quadrant. Their prediction that the galactic equivalent of a solar coronal hole exists in the SW quadrant may be supported by the PSPC data. Their prediction is based upon the minimum in the polarization data coupled with an excess Faraday rotation measure. The X-ray data shown an apparent asymmetry in the distribution of the X-ray emission north-south about the nucleus. The southern portion appears to be deficient relative to the north side. Making this qualitative statement quantitative is difficult due to the dominance of the point sources. An attempt has been made however. Wedges with an opening angle of 45° and lying along the major axis of NGC 6946 define the profiles. Annuli lying within the wedges of width $16''$ have been used to extract the counts from the background-subtracted image (i.e., Fig. 4). Figure 10 shows

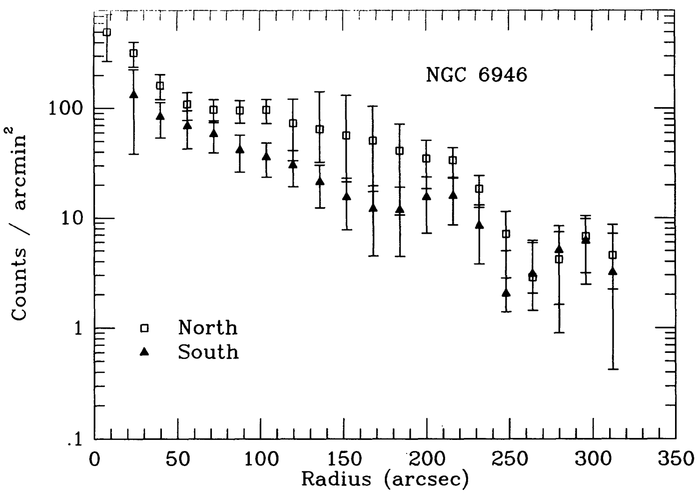

FIG. 10.—Radial profiles in 45° wedges centered on the major axis of NGC 6946. The north profile consistently lies above the southern profile, although the evidence for a distinct difference is weak.

the results. The evidence for a deficit in the southern wedge is weak, although the southern wedge profile does lie consistently below the northern profile. Unfortunately, the SW region is rather chaotic in other bands, rendering it difficult to understand the situation. As mentioned, Ehle & Beck (1993) find the magnetic field lines perpendicular to the disk in this region, derived from the higher polarization and steeper pitch angles present in their data. Tacconi & Young (1990) suggest the density wave potential is broader in this area, resulting in less-sharply defined spiral arms. Their suggestion is based upon their *B*- and *I*-band observations of the arm-interarm contrasts. Even an H I map (Boulanger & Viallefond 1992) does not show sharp spiral arms in the SW region. In fact, the two western arms appear to merge in the SW region, although the apparent merger could be a contrast effect, with the inner western arm joining the nuclear region north of the apparent merge area. Optically, it is also not clear what the situation in the SW region is. An Hα map in Devereaux & Young (1993) or Ehle & Beck (1993) does not provide much additional insight. Based upon the X-ray data, I regard the Ehle & Beck suggestion as interesting, but requiring further data to establish or refute definitively.

As a final comment, I note that the integrated X-ray properties of NGC 6946 have long been known to be softer than the average spiral galaxy (FT). Correlations have been made between X-ray properties and integrated properties from other bandpasses. Given that source S1 so dominates the X-ray emission from NGC 6946, it is a point of concern that the correlations may, in some cases, be exceedingly sensitive to particular bright sources. Certainly, comparing integrated properties is a valid scientific goal; however, I believe the NGC 6946 results indicate the need for caution in doing so.

6. SUMMARY

The *ROSAT* PSPC data on the nearby spiral galaxy NGC 6946 has been presented. The data show that the *Einstein* IPC "nuclear source" is composed of approximately three sources. The source on the north arm, barely resolved from the nuclear source by *Einstein*, is well resolved and identified as a probable supernova remnant (Schlegel 1994a). A total of nine sources are present above a flux of $\sim 10^{37.1}$ ergs s^{-1}. X-ray spiral structure is clearly present, particularly for the optically prominent northeastern arm, indicating the X-rays at least arise from a source distributed along the arms. No X-ray "corona" or halo is obvious from the PSPC data, although the X-ray emissivity does appear to match the results from other wavelength bands in the SW region of the galaxy. The diffuse emission appears to be truly diffuse and not the summed emission of point sources.

I thank the referee for helpful comments that improved this paper. This research was aided by the use of the NASA Extragalactic Database. I also thank D. Davis for obtaining the optical image of NGC 6946.

REFERENCES

Arp, H. 1966, Atlas of Peculiar Galaxies (Pasadena: Caltech)
Beck, R. 1991, A&A, 251, 15
Blair, W., & Fesen, R. 1994. ApJ, 424, L103
Boulanger, F., & Viallefond, F. 1992, A&A, 266, 37
Burstein, D., & Heiles, C. 1984, ApJS, 54, 33
de Gioia-Eastwood, K., Grasdalen, G. L., & Strom, K. M. 1984, ApJ, 278, 564
Devereaux, N., & Young, J. 1993, AJ, 106, 948
Ehle, M., & Beck, R. 1993, A&A, 273, 45
Engargiola, G. 1991, ApJS, 76, 875
Fabbiano, G. 1989, ARA&A, 27, 87
———. 1992, in X-ray Binaries, ed. W. Lewin, J. van Paradijs, & E. van den Heuvel (Cambridge: Cambridge Univ. Press)
Fabbiano, G., Feigelson, E., & Zamorani, G. 1982, ApJ, 256, 397
Fabbiano, G., Gioia, I., & Trinchieri, G. 1988, ApJ, 324, 749
Fabbiano, G., & Trichieri, G. 1987, ApJ, 315, 46 (FT)
Giuricin, G., Bertotti, G., Mardiossian, F., & Mezzetti, M. 1991, MNRAS, 250, 392
Hasinger, G., Schmidt, M., & Trümper, J. 1991, A&A, 246, L2
Hasinger, G., Turner, T., George, I., & Boese, G. 1992, *ROSAT* Calibration Memo. 92-001
Ishizuki, S., Kawabe, R., Ishiguro, M., Okumura, S., Morita, M.-I., Chikada, Y., Kasuga, T., & Doi, M. 1990, ApJ, 355, 436
Israel, P. F. 1980, A&A, 90, 246
Kamphius, J., & Sancisi, R. 1993, A&A, 273, L31
Kim, D.-W., Fabbiano, G., & Trinchieri, G. 1992, ApJS, 80, 645
Klein, U., Beck, R., Buczilowski, U. R., & Wielebinski, R. 1982, A&A, 108, 176
Kürster, M., & Hasinger, G. 1993, Internal MPE Memo., March 10
Long, K., Gordon, S., Blair, W., & Charles, P. 1994, in The Soft X-Ray Cosmos, ed. E. M. Schlegel & R. Petre (New York: AIP), 339
McCall, M. L. 1982, Ph.D. thesis, Univ. Texas at Austin
Madden, S. C., Geis, N., Genzel, R., Herrmann, F., Jackson, J., Poglitsch, A., Stacey, G. J., & Townes, C. H. 1993, ApJ, 407, 579
Nousek, J., & Lesser, A. 1993, US *ROSAT* Newsletter, 8, 13
Pfeffermann, E., et al. 1986, Proc. SPIE, 733, 519
Primini, F., Forman, W., & Jones, C. 1993, ApJ, 410, 615
Rogstad, D. H., Shostak, G. S., & Rots, A. H. 1973, A&A, 22, 111
Roy, J.-R., & Belley, J. 1993, ApJ, 406, 60
Schlegel, E. M. 1994a. ApJ, 424, L99
———. 1994b, AJ, submitted
Snowden, S., McCammon, D., Burrows, D., & Mendenhall, J. 1994, ApJ, 424, 714
Snowden, S., Plucinsky, P., Briel, U., Hasinger, G., & Pfeffermann, E. 1992, ApJ, 393, 819
Tacconi, L. J., & Young, J. S. 1990, ApJ, 352, 595
Telesco, C. M., & Harper, D. A. 1980, ApJ, 235, 392
Trinchieri G., Fabbiano, G., & Palumbo, G. 1985, ApJ, 290, 96
Trinchieri, G., Fabbiano, G., & Peres, G. 1988, ApJ, 325, 531
Trümper, J., et al. 1991, Nature, 349, 579
Tully, R. 1988, Nearby Galaxies Catalog (Cambridge: Cambridge Univ. Press)
van der Kruit, P. C., Allen, R. J., & Rots, A. H. 1977, A&A, 55, 421
VanDyk, S., et al. 1994, ApJ, 425, L77
Wang, Q. D. 1993, in Star Formation, Galaxies, and the Interstellar Medium, ed. J. Franco, F. Ferrini, & G. Tenorio-Tagle (Cambridge: Cambridge Univ. Press), 56
Wang, Q., Hamilton, T., & Helfand, D. 1989, Nature, 341, 309
Wang, Q., Hamilton, T., Helfand, D., & Wu, X. 1991, ApJ, 374, 475
Young, J., & Scoville, N. 1982, ApJ, 258, 467